Flow over bodies with suction through porous strips

A. H. Nayfeh, H. L. Reed, and S. A. Ragab

Citation: Physics of Fluids (1958-1988) **29**, 2042 (1986); doi: 10.1063/1.865590
View online: http://dx.doi.org/10.1063/1.865590
View Table of Contents: http://scitation.aip.org/content/aip/journal/pof1/29/7?ver=pdfcov
Published by the AIP Publishing

Flow over bodies with suction through porous strips

A. H. Nayfeh, H. L. Reed,[a] and S. A. Ragab
Department of Engineering Science and Mechanics, Virginia Polytechnic Institute and State University, Blacksburg, Virginia 24061

(Received 8 October 1985; accepted 14 April 1986)

This article addresses the steady, incompressible flow past a two-dimensional or an axisymmetric body with suction through porous strips. Closed-form solutions for each flow quantity are developed in the context of linearized triple-deck theory using Fourier transforms. To demonstrate the validity of these closed-form solutions, we compare the wall shear stress and pressure coefficients and the streamwise velocity profiles from the linearized theory are compared with those obtained by the numerical integration of both interacting and conventional boundary-layer equations. The agreement between the linearized triple-deck and interacting boundary-layer equations for the suction configurations proposed for laminar flow control is good; however, the conventional boundary layers, which fail to account for upstream influence, are shown to be in poor agreement with both interacting boundary layers and the linearized triple deck. Combining these linearized closed-form solutions with a perturbation scheme has enabled development of a simple linear optimization scheme to determine the number, spacing, and mass flow rate through the strips on two-dimensional and axisymmetric bodies.

I. INTRODUCTION

One of the approaches proposed for laminar flow control is suction through porous strips. To determine the effectiveness of such an approach and to optimize the number, spacing, and flow rate through such strips, one needs to determine the stability of the flow over a body with suction strips. The first step in such an approach is the calculation of the mean flow. Nayfeh and El-Hady[1] used a conventional boundary-layer code. However, conventional boundary-layer calculations fail to account for the upstream influence (deviation in pressure gradient). In this work, we present a linearized triple-deck, closed-form solution, which is more efficient and requires much less computer time. Consequently, it is ideal for optimization of the suction distribution for laminar flow control.[2,3] The linearized triple-deck equations are expected to be valid only for suction levels $O(\mathrm{Re}^{-3/8} U_\infty^*)$, so we will demonstrate their validity for suction levels the order of those proposed for laminar flow control by comparison of their solutions with those of interacting boundary-layer equations. In fact, the stability of the flow calculated using the present formulation[2] are in good agreement with the experimental results of Reynolds and Saric.[4]

Although numerical techniques now exist to treat most nonlinear triple-deck and interacting boundary-layer equations, a closed form solution for the triple-deck equations is a valuable tool for determining the optimum suction configuration. In the nonlinear case, one needs to solve for the mean flow whenever any parameter, such as the number, spacing, and flow rate, is changed. This requires a great deal of computer time. On the other hand, if the problem can be linearized and a closed form solution is obtained, one can couple this solution with a perturbation method to develop a simple optimization scheme to determine the number, spacing, and flow rate through such strips. Such a scheme was developed in Refs. 2 and 3 for axisymmetric and two-dimensional bodies, respectively. The results for flat plates[2] are in excellent agreement with the experimental results of Reynolds and Saric.[4]

Laminar viscous flow over a two-dimensional or an axisymmetric body with suction exhibits a triple-deck structure.[5–8] This is shown schematically in Fig. 1. Upstream of the region influenced by the suction is the Prandtl boundary layer. The flow in the neighborhood of the porous strip centered at x_r^* is described by three decks or nested boundary layers. The middle deck, the displaced Prandtl layer, whose thickness is $O(\mathrm{Re}^{-1/2} x_r^*)$, is characterized by rotational, inviscid disturbances. The upper deck, whose thickness is $O(\mathrm{Re}^{-3/8} x_r^*)$, has inviscid, irrotational disturbances. The lower deck, whose thickness is $O(\mathrm{Re}^{-5/8} x_r^*)$, has viscous, rotational disturbances. The wall boundary conditions are satisfied by the lower-deck governing equations.

For the case of blowing, Napolitano and Messick[9] developed a closed-form solution for the linearized lower-deck equations and calculated only the wall pressure and shear stress. In this article, we obtain a linear triple-deck solution for one finite-length strip, and then we appeal to the linearity of the problem and use superposition to obtain a closed-form solution for any number of strips. The region around the strip to be studied is expanded in triple-deck variables and the mean flow is taken to be the flow over the suctionless body plus a perturbation resulting from all upstream strips. Moreover, we determine a composite expansion for the flow that is valid everywhere for stability calculations.

II. LINEARIZED TRIPLE-DECK THEORY

In this section we derive the governing equations of linearized first-order, triple-deck theory for an adiabatic flat plate or axisymmetric body with porous strips. Rather than stating the nonlinear triple-deck equations and then carrying

[a] Present address: Department of Mechanical and Aerospace Engineering, Arizona State University, Tempe, Arizona 85287.

 0031-9171/86/072042-12$01.90

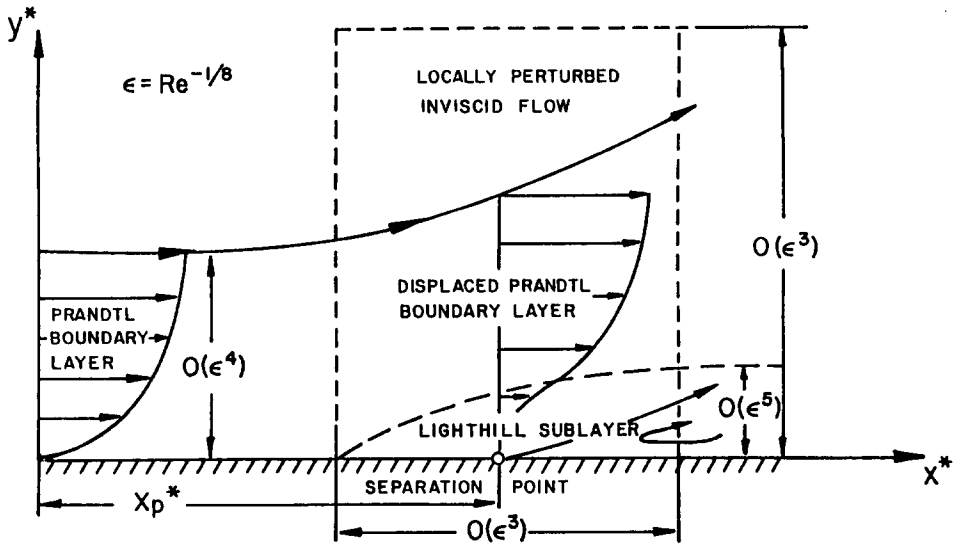

FIG. 1. Schematic of the triple deck structure near a disturbance point.

out the linearization, we linearize the Navier–Stokes equations, introduce a stretching transformation, and determine the distinguished limits that clearly exhibit the triple-deck structure. We solve the lower-deck equations analytically to obtain closed-form solutions for each flow variable. Then, we use the method of composite expansions to obtain a solution for the flow past one strip. Next, by appealing to the linearity of the problem, we use superposition to obtain a composite solution for the flow past many strips.

A. Basic state

Considering incompressible, steady two-dimensional or axisymmetric flow past a body, we define the coordinate system (x^*, y^*, θ) shown in Fig. 2 and denote the local radius of the body measured from the axis as $r_0^*(x^*)$, where all starred quantities are dimensional. To determine the boundary-layer equations describing the flow past the suctionless body, we define a Reynolds number at a reference location x_r^* as $\mathrm{Re} = U_\infty^* x_r^*/\nu^*$ and introduce the following dimensionless variables:

$$u = \frac{u^*}{U_\infty^*}, \quad v = \frac{v^*}{U_\infty^*}, \quad p = \frac{p^* - p_\infty^*}{\rho^* U_\infty^{*2}},$$
$$x = \frac{x^*}{x_r^*}, \quad y = \frac{y^*}{x_r^*}, \quad r_0 = \frac{r_0^*}{x_r^*}, \tag{1}$$

where ∞ denotes free-system conditions, u and v are the velocity components tangent to and normal to the surface, respectively, and p is the pressure. Assuming r_0^* to be much larger than the boundary-layer thickness (i.e., the transverse-curvature effects are negligible), one finds the following boundary-layer equations governing the flow without suction:

$$\frac{\partial}{\partial x}(r_0^m U) + r_0^m \frac{\partial v}{\partial y} = 0, \tag{2a}$$

$$U\frac{\partial U}{\partial x} + v\frac{\partial U}{\partial y} = -\frac{dP}{dx} + \frac{1}{\mathrm{Re}}\frac{\partial^2 U}{\partial y^2}, \tag{2b}$$

$$U = v = 0, \quad \text{at } y = 0, \tag{2c}$$

$$U \to U_e, \quad \text{as } y \to \infty, \tag{2d}$$

where $m = 0$ for two-dimensional flows and $m = 1$ for axisymmetric flows and $U_e = U_e^*/U_\infty^*$.

To generate the boundary-layer flow for a given geometry, one needs to solve the inviscid problem past the suctionless body to determine U_e and hence P and then to integrate Eqs. (2). The end result is

$$u^*/U_\infty^* = U(x, y\epsilon^{-4}), \quad v^*/U_\infty^* = \epsilon^4 V(x, y\epsilon^{-4}),$$
$$(p^* - p_\infty^*)/\rho^* U_\infty^{*2} = P(x), \tag{3a}$$

where

$$\epsilon = \mathrm{Re}^{-1/8}, \quad \mathrm{Re} = U_\infty^* x_r^*/\nu^*. \tag{3b}$$

B. Disturbance equations

If a small disturbance, such as a porous strip having the uniform suction level v_w^*, is introduced at $x^* = x_r^*$, then the flow field in its neighborhood is perturbed and can be expressed as

$$u^*/U_\infty^* = U(x, y\epsilon^{-4}) + v_w u(x, y), \tag{4a}$$

$$v^*/U_\infty^* = \epsilon^4 V(x, y\epsilon^{-4}) + v_w v(x, y), \tag{4b}$$

$$(p^* - p_\infty^*)/\rho^* U_\infty^{*2} = P(x) + v_w p(x, y), \tag{4c}$$

where $v_w^* = \epsilon^3 U_\infty^* v_w$. Substituting Eqs. (4) into the Navier–Stokes equations, subtracting the basic-state quantities, assuming the longitudinal curvature to be small, and keeping linear terms in the perturbation quantities, we obtain

$$\frac{\partial}{\partial x}[(r_0 + y)^m u] + \frac{\partial}{\partial y}[(r_0 + y)^m v] = 0, \tag{5a}$$

$$U\frac{\partial u}{\partial x} + v\frac{\partial U}{\partial y} + u\frac{\partial U}{\partial x} + \epsilon^4 V\frac{\partial u}{\partial y} = -\frac{\partial p}{\partial x} + \epsilon^8\left(\frac{\partial^2 u}{\partial x^2} + \frac{\partial^2 u}{\partial y^2}\right), \tag{5b}$$

$$U\frac{\partial v}{\partial x} + \epsilon^4 u\frac{\partial V}{\partial x} + \epsilon^4 v\frac{\partial V}{\partial y} + \epsilon^4 V\frac{\partial v}{\partial y}$$

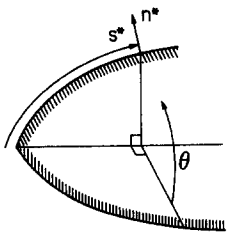

FIG. 2. Coordinate system.

$$= -\frac{\partial p}{\partial y} + \epsilon^8\left(\frac{\partial^2 v}{\partial x^2} + \frac{\partial^2 v}{\partial y^2}\right). \tag{5c}$$

The boundary conditions at the wall are

$$u(x,0) = 0, \tag{5d}$$

$$v(x,0) = \begin{cases} \epsilon^3, & \text{for } x_{\rm LE} \leqslant x \leqslant x_{\rm TE}, \\ 0, & \text{otherwise}, \end{cases} \tag{5e}$$

where $x_{\rm LE}$ and $x_{\rm TE}$ are the leading and trailing edges of the strip. The effect of the perturbation must decay away from the wall and the suction strip so that

$$u(x,y),\quad v(x,y),\quad p(x,y) \to 0,\quad \text{as } x \to \pm\infty, \tag{5f}$$

$$u(x,y),\quad v(x,y),\quad p(x,y) \to 0,\quad \text{as } y \to \infty. \tag{5g}$$

C. Expansions

As $\epsilon \to 0$, the reduced equations [(5a)–(5c)] cannot satisfy all boundary conditions at the wall and an expansion or expansions valid near the wall must be introduced. To accomplish this, a stretching transformation

$$Y_n = \epsilon^{-n} y, \tag{6a}$$

where n is an integer, is introduced. Triple-deck theory shows that the effect of the strip occurs in a neighborhood of

$$x^* = x_r^*(1 + \epsilon^3 X), \tag{6b}$$

where $X = O(1)$. We assume that the radius r_0 of the body is greater than or equal to the order of ϵ^3. Thus, we put $r_0 = R_0\epsilon^3$, where $R_0 \geqslant O(1)$. Substituting Eqs. (6) into Eqs. (5a)–(5c) yields

$$\frac{\partial}{\partial X}\{[R_0(1+\epsilon^3 X) + \epsilon^{n-3} Y_n]^m u\} + \epsilon^{3-n}\frac{\partial}{\partial Y_n} \times \{[R_0(1+\epsilon^3 X) + \epsilon^{n-3} Y_n]^m v\} = 0, \tag{7a}$$

$$U(1+\epsilon^3 X, \epsilon^{n-4} Y_n)\frac{\partial u}{\partial X} + \epsilon^{3-n} v\frac{\partial}{\partial Y_n} \times [U(1+\epsilon^3 X, \epsilon^{n-4} Y_n)] + u\frac{\partial}{\partial X}[U(1+\epsilon^3 X, \epsilon^{n-4} Y_n)] + \epsilon^{7-n} V\frac{\partial u}{\partial Y_n} = -\frac{\partial p}{\partial X} + \epsilon^5\frac{\partial^2 u}{\partial X^2} + \epsilon^{11-2n}\frac{\partial^2 u}{\partial Y_n^2}, \tag{7b}$$

$$U(1+\epsilon^3 X, \epsilon^{n-4} Y_n)\frac{\partial v}{\partial X} + \epsilon^4 u\frac{\partial}{\partial X}[V(1+\epsilon^3 X, \epsilon^{n-4} Y_n)] + \epsilon^{7-n} v\frac{\partial}{\partial Y_n}[V(1+\epsilon^3 X, \epsilon^{n-4} Y_n)] + \epsilon^{7-n} V(1+\epsilon^3 X, \epsilon^{n-4} Y_n)\frac{\partial v}{\partial Y_n} = -\epsilon^{3-n}\frac{\partial p}{\partial Y_n} + \epsilon^5\frac{\partial^2 v}{\partial X^2} + \epsilon^{11-2n}\frac{\partial^2 v}{\partial Y_n^2}. \tag{7c}$$

Letting $\epsilon \to 0$ with X and Y_n being fixed, we find from Eq. (7a) that

$$v = O(\epsilon^{n-3} u)$$

and

$$(R_0 + \epsilon^{n-3} Y_n)^m\frac{\partial u}{\partial X} + \epsilon^{3-n}\frac{\partial}{\partial Y_n}[(R_0 + \epsilon^{n-3} Y_n)^m v] = 0. \tag{7d}$$

To determine the limits of Eqs. (7b) and (7c) as $\epsilon \to 0$, we note that

$$\lim_{\epsilon\to 0} U(1+\epsilon^3 X, \epsilon^{n-4} Y_n) = \begin{cases} \epsilon^{n-4}\lambda Y_n, & \text{if } n > 4, \\ U(Y_4), & \text{if } n = 4, \\ U_e(1), & \text{if } n < 4, \end{cases} \tag{8a}$$

where

$$\lambda = \frac{\partial U}{\partial Y_4}(1,0), \quad U(Y_4) = U(1, Y_4). \tag{8b}$$

Hence, letting $\epsilon \to 0$ in Eqs. (7b) and (7c), we find three distinguished limits corresponding to $n = 3, 4$, and 5, respectively. The limit corresponding to $n = 3$ is usually called the upper deck, the limit corresponding to $n = 4$ is called the middle deck, and the limit corresponding to $n = 5$ is called the lower deck.

1. The lower deck

In this case, $n = 5$ and it follows from Eqs. (5e) and (7d) that the lower deck variables (denoted by superscript l) can be expanded as

$$u^l = \epsilon\tilde{u}(X, Y_5) + \cdots, \quad v^l = \epsilon^3\tilde{v}(X, Y_5) + \cdots, \quad p^l = \epsilon^2\tilde{p}(X, Y_5) + \cdots. \tag{9}$$

Substituting Eqs. (9) into Eqs. (7b)–(7d) and (5d)–(5g), we obtain

$$\frac{\partial\tilde{u}}{\partial X} + \frac{\partial\tilde{v}}{\partial Y_5} = 0, \tag{10a}$$

$$\lambda Y_5\frac{\partial\tilde{u}}{\partial X} + \lambda\tilde{v} = -\frac{\partial\tilde{p}}{\partial X} + \frac{\partial^2\tilde{u}}{\partial Y_5^2}, \tag{10b}$$

$$\frac{\partial\tilde{p}}{\partial Y_5} = 0 \quad \text{or} \quad \tilde{p} = \tilde{p}(X), \tag{10c}$$

$$\tilde{u}(X,0) = 0, \quad \tilde{u}(-\infty, Y_5) = 0, \quad \tilde{p}(-\infty) = 0, \tag{10d}$$

$$\tilde{v}(X,0) = \begin{cases} 1, & \text{for } \tilde{X}_{\rm LE} \leqslant X \leqslant \tilde{X}_{\rm TE}, \\ 0, & \text{otherwise}. \end{cases} \tag{10e}$$

The other boundary conditions are provided by matching the lower and middle decks.

2. The middle deck

In this case, $n = 4$ and it follows from Eqs. (7d) and matching with the lower deck that the middle-deck variables can be expanded as

$$u^m = \epsilon u_1 + \cdots, \quad v^m = \epsilon^2 v_2 + \cdots, \quad p^m = \epsilon^2 p_2 + \cdots. \tag{11}$$

Substituting Eqs. (11) into Eqs. (7b)–(7d), we find that

$$\frac{\partial u_1}{\partial X} + \frac{\partial v_2}{\partial Y_4} = 0, \tag{12a}$$

$$U(Y_4)\frac{\partial u_1}{\partial X} + v_2 U'(Y_4) = 0, \tag{12b}$$

$$\frac{\partial p_2}{\partial Y_4} = 0. \tag{12c}$$

Solving Eqs. (12a)–(12c) and substituting the result into Eqs. (11), we have

$$u^m = \epsilon U'(Y_4)A(X) + \cdots, \tag{13a}$$

$$v^m = -\epsilon^2 U(Y_4)\frac{dA}{dX} + \cdots, \tag{13b}$$

$$p^m = \epsilon^2 p_2(X) + \cdots, \tag{13c}$$

where $A(X) \to 0$ as $x \to -\infty$ according to Eq. (5f). Matching the lower and middle decks yields

$$\lim_{Y_5 \to \infty} \tilde{u}(X, Y_5) = \lambda A(X), \tag{14a}$$

$$p_2(X) = \tilde{p}(X), \tag{14b}$$

$$\lim_{Y_5 \to \infty} \tilde{v}(X, Y_5) = -\lambda Y_5 \frac{dA}{dX}. \tag{14c}$$

3. The upper deck

In this case, $n = 3$ and it follows from Eqs. (7d) and matching with the middle deck that the upper-deck variables can be expanded as

$$u^u = \epsilon^2 \hat{u}_2 + \cdots, \quad v^u = \epsilon^2 \hat{v}_2 + \cdots, \quad p^u = \epsilon^2 \hat{p}_2 + \cdots. \tag{15}$$

Substituting Eqs. (15) into Eqs. (7b)–(7d), (5f), and (5g) yields

$$\frac{\partial \hat{u}_2}{\partial X} + \frac{\partial \hat{v}_2}{\partial Y_3} + \frac{m\hat{v}_2}{R_0 + Y_3} = 0, \tag{16a}$$

$$\frac{\partial \hat{u}_2}{\partial X} + \frac{\partial \hat{p}_2}{\partial X} = 0, \tag{16b}$$

$$\frac{\partial \hat{v}_2}{\partial X} + \frac{\partial \hat{p}_2}{\partial Y_3} = 0, \tag{16c}$$

$$\hat{v}_2(X, \infty) = 0, \quad \hat{v}_2(\pm\infty, Y_3) = 0. \tag{16d}$$

Matching the upper and middle decks yields

$$\hat{u}_2(X,0) = 0, \quad \hat{v}_2(X,0) = -U_e \frac{dA}{dX},$$

$$\hat{p}_2(X,0) = p_2(X). \tag{16e}$$

When $R_0 \gg O(1)$, the last term in Eq. (16a) can be neglected and consequently the triple-deck solution for the axisymmetric body is the same as that for a two-dimensional body. In this case, the solution of Eqs. (16) is[10]

$$\hat{v}_2 = -\frac{Y_3 U_e}{\pi}\int_{-\infty}^{\infty} \frac{A'(t)}{(X-t)^2 + Y_3^2}\,dt, \tag{17a}$$

$$\hat{p}_2 = \frac{U_e}{\pi}\int_{-\infty}^{\infty} \frac{(X-t)A'(t)}{(X-t)^2 + Y_3^2}\,dt. \tag{17b}$$

It follows from Eqs. (14b), (16e), and (17b) that

$$p_2(X) = \tilde{p}(X) = \frac{U_e}{\pi}\int_{-\infty}^{\infty} \frac{A'(t)}{X-t}\,dt. \tag{18a}$$

Inverting Eq. (18a) yields

$$\frac{dA}{dX} = -\frac{1}{\pi U_e}\int_{-\infty}^{\infty} \frac{p_2(t)}{X-t}\,dt. \tag{18b}$$

Differentiating Eq. (18b) with respect to X and using integration by parts yields

$$\frac{d^2A}{dX^2} = -\frac{1}{\pi U_e}\int_{-\infty}^{\infty} \frac{p_2'(t)}{X-t}\,dt. \tag{18c}$$

When $R_0 = O(1)$, the solution of Eqs. (16a)–(16e) is given by Duck.[11] In this article, we restrict our analysis to the case $R_0 \gg O(1)$.

III. SOLUTION OF LOWER-DECK PROBLEM

To solve the lower-deck problem, we introduce the following transformation that eliminates the dependence of the lower-deck variables on the free-stream conditions:

$$\tilde{u} = \lambda^{-1/2} U_e^{1/2} \bar{u}(\bar{x}, \bar{y}), \quad \tilde{v} = \bar{v}(\bar{x}, \bar{y}),$$

$$\tilde{p} = \lambda^{-1/4} U_e^{3/4} \bar{p}(\bar{x}),$$

$$A = \lambda^{-3/2} U_e^{1/2} \delta(\bar{x}), \quad X = \lambda^{-5/4} U_e^{3/4} \bar{x},$$

$$Y_5 = \lambda^{-3/4} U_e^{1/4} \bar{y}. \tag{19}$$

Then, the lower-deck problem becomes

$$u_x + v_y = 0, \tag{20a}$$

$$yu_x + v = -p' + u_{yy}, \tag{20b}$$

$$u(x,0) = 0, \tag{20c}$$

$$v(x,0) = \begin{cases} 1, & \text{for } x_{LE} \leqslant x \leqslant x_{TE}, \\ 0, & \text{otherwise}, \end{cases} \tag{20d}$$

$$u(x,\infty) = \delta, \tag{20e}$$

$$u(-\infty, y) = 0, \tag{20f}$$

$$\delta_{xx} = -\frac{1}{\pi}\int_{-\infty}^{\infty} \frac{p'(t)}{x-t}\,dt, \tag{20g}$$

$$p(\pm\infty) = 0, \tag{20h}$$

where the overbar was dropped for convenience in notation.

First, we consider a semi-infinite strip with leading edge at $x = 0$. Because the system [(20a) and (20b)] is linear, solutions for finite-length strips can be obtained by translations and superpositions of semi-infinite solutions. We use the subscript ∞ to indicate semi-infinite solutions. For the semi-infinite problem, the boundary condition (20d) becomes

$$v_\infty(x,0) = H(x), \tag{21}$$

where $H(x)$ is the Heaviside function. To solve the resulting

problem, we differentiate Eq. (20b) with respect to y, apply Eq. (20a) and obtain

$$yu_{\infty xy} - u_{\infty yyy} = 0. \tag{22}$$

If we let $w = u_{\infty y}$, then

$$w_{yy} - yw_x = 0. \tag{23}$$

We define the Fourier transform in x of any dependent variable $r(x)$ by

$$R(\omega) = \lim_{\alpha \to 0^+} \int_{-\infty}^{\infty} r(x) e^{-(i\omega + \alpha)x}\, dx,$$
$$r(x) = \frac{1}{2\pi} \lim_{\alpha \to 0^+} \int_{-\infty}^{\infty} R(\omega) e^{(i\omega + \alpha)x}\, d\omega. \tag{24}$$

Since u_∞, v_∞, p_∞, and δ_∞ all tend to zero as $x \to -\infty$, the first integral always converges at the lower limit. Using a limit process, one can show that the integral converges at the upper limit when $0 < \alpha \ll 1$. We use the capital letter to indicate the Fourier transform of the corresponding small letter. Using complex variables and defining the polar form of ω as $|\omega| \exp(i\phi)$, we find that the only nonintegral powers of $i\omega$ involve the cubic root. The most convenient branch for these turns out to be

$$(i\omega)^{1/3} = |\omega|^{1/3} \exp\left[\tfrac{1}{3} i(\phi + \tfrac{1}{2}\pi)\right],$$

where $-3\pi/2 < \phi < \pi/2$.

Applying the Fourier transform in x to Eq. (23) gives Airy's equation

$$W_{yy} - i\omega y W = 0, \tag{25}$$

whose solution subject to the condition (20e) is[12]

$$W = c_1 \operatorname{Ai}[(i\omega)^{1/3} y], \tag{26}$$

where c_1 is a constant.

Integrating Eq. (26) with respect to y, using Eq. (20c), and recalling the fact that $W = U_y$, we obtain

$$U = c_1 \int_0^y \operatorname{Ai}[(i\omega)^{1/3} t\,]\, dt. \tag{27}$$

Using Eq. (27) in the Fourier transform of Eq. (20e) gives

$$\Delta = c_1 \int_0^{\infty} \operatorname{Ai}[(i\omega)^{1/3} t\,]\, dt = \frac{c_1}{3(i\omega)^{1/3}}.$$

Hence

$$c_1 = 3(i\omega)^{1/3} \Delta. \tag{28}$$

Taking the Fourier transform of Eq. (20g) gives

$$\omega \Delta = P \operatorname{sgn} \omega. \tag{29}$$

When $y = 0$, Eqs. (20b) and (21) give

$$H(x) + p_{\infty x} = u_{\infty yy}(x,0)$$

whose Fourier transform yields

$$1/i\omega + i\omega P = U_{yy}(\omega,0). \tag{30}$$

Equations (27) and (30) give

$$i\omega P + 1/i\omega = c_1 \operatorname{Ai}'(0)(i\omega)^{1/3}. \tag{31}$$

The solution of Eqs. (28), (29), and (31) is

$$P = -(i\omega)^{-2/3}/D, \tag{32a}$$
$$c_1 = -3i(i\omega)^{-4/3}(\operatorname{sgn}\omega/D), \tag{32b}$$
$$\Delta = -[i(i\omega)^{-5/3}/D]\operatorname{sgn}\omega, \tag{32c}$$

where

$$D = (i\omega)^{4/3} + i\theta^{4/3} \operatorname{sgn}\omega,$$
$$\theta = [-3 \operatorname{Ai}'(0)]^{3/4} \tag{33}$$

is Lighthill's constant.

In the next three sections, we invert the Fourier transforms to find p_∞, u_∞, and δ_∞, respectively.

A. Lower-deck pressure

The inverse transform of Eq. (32a) gives

$$p_\infty = -\frac{1}{2\pi} \int_{-\infty}^{\infty} \frac{(i\omega)^{-2/3}}{(i\omega)^{4/3} + i\theta^{4/3} \operatorname{sgn}\omega} e^{i\omega x}\, d\omega,$$

which upon letting $\omega = r^3\theta$ becomes

$$p_\infty = -\frac{3}{2\pi\theta} \int_0^{\infty} \frac{e^{ir^3\theta x}\, dr}{-r^4 + e^{i5\pi/6}} - \frac{3}{2\pi\theta} \int_0^{\infty} \frac{e^{-ir^3\theta x}\, dr}{-r^4 + e^{-i5\pi/6}}. \tag{34}$$

For $x < 0$, Eq. (34) can be rewritten as

$$p_\infty = -\frac{3}{2\pi\theta} \int_0^{\infty} \frac{e^{-ir^3\theta|x|}}{-r^4 + e^{i5\pi/6}}\, dr - \frac{3}{2\pi\theta} \int_0^{\infty} \frac{e^{ir^3\theta|x|}}{-r^4 + e^{-i5\pi/6}}\, dr. \tag{35}$$

To evaluate each of these two integrals, we appeal to Cauchy's residue theorm. For the first integral in Eq. (35), we consider the closed contour $C = C_1 \cup C_2 \cup C_3$, where $C_1 = [0,R]$, $C_2 = [r | r\epsilon$ circular arc from R to $R \exp(-i\pi/6)]$, and $C_3 = [R \exp(-i\pi/6), 0]$. As $R \to \infty$, the integral over the contour C_2 vanishes so that

$$\int_0^{\infty} \frac{e^{-ir^3\theta|x|}}{-r^4 + e^{i5\pi/6}}\, dr = \int_0^{\infty e^{-i\pi/6}} \frac{e^{-ir^3\theta|x|}}{-r^4 + e^{i5\pi/6}}\, dr. \tag{36a}$$

For the second integral in Eq. (35), we consider the closed contour consisting of $[0,R]$, $[r | r\epsilon$ circular arc from R to $R \exp(i\pi/6)]$, and $[R \exp(i\pi/6), 0]$. As $R \to \infty$, the integral over the circular arc vanishes so that

$$\int_0^{\infty} \frac{e^{ir^3\theta|x|}}{-r^4 + e^{-i5\pi/6}}\, dr = \int_0^{\infty e^{i\pi/6}} \frac{e^{ir^3\theta|x|}}{-r^4 + e^{-i5\pi/6}}\, dr. \tag{36b}$$

Using Eqs. (36a) and (36b) in Eq. (35), we have

$$p_\infty = -\frac{3}{2\pi\theta} \int_0^{\infty e^{-i\pi/6}} \frac{e^{-ir^3\theta|x|}}{-r^4 + e^{i5\pi/6}}\, dr - \frac{3}{2\pi\theta} \int_0^{\infty e^{i\pi/6}} \frac{e^{ir^3\theta|x|}}{-r^4 + e^{-i5\pi/6}}\, dr. \tag{37}$$

Letting $\rho = r \exp(i\pi/6)$ in the first integral and $\rho = r \times \exp(-i\pi/6)$ in the second integral and combining these two integrals, we obtain

$$p_\infty = \frac{3}{\pi\theta} \int_0^{\infty} \frac{1}{\rho^8 + 1} e^{-\rho^3\theta|x|}\, d\rho, \quad \text{for } x < 0. \tag{38}$$

For $x > 0$, following a reasoning similar to that in the case $x < 0$, we obtain

$$p_\infty = \frac{3}{2\pi\theta}\int_0^\infty \frac{1}{\rho^8 - \sqrt{3}\rho^4 + 1} e^{-\rho^3\theta x}\, d\rho, \quad \text{for } x > 0. \tag{39}$$

Equations (38) and (39) are essentially the same as those of Napolitano and Messick.[9]

B. Lower-deck δ_∞

The inverse transform of Eq. (32c) gives

$$\delta_\infty = \frac{1}{2\pi}\lim_{\alpha\to 0^+}\int_{-\infty - i\alpha}^{\infty - i\alpha} \frac{-i(i\omega)^{-5/3}\,\mathrm{sgn}\,\omega}{(i\omega)^{4/3} + \theta^{4/3} i\,\mathrm{sgn}\,\omega} e^{i\omega x}\, d\omega. \tag{40}$$

We note that the integrand in Eq. (40) has a branch point at the origin in addition to the branch cut. This is the reason we exhibited explicitly the limit $\alpha\to 0^+$ in the inverse transform. Using partial fractions, we rewrite Eq. (40) as

$$\delta_\infty = I_1 + I_2, \tag{41}$$

where

$$I_1 = -\frac{1}{2\pi}\lim_{\alpha\to 0^+}\int_{-\infty - i\alpha}^{\infty - i\alpha} \frac{e^{i\omega x}\, d\omega}{(i\omega)^{5/3}\theta^{4/3}}, \tag{42}$$

$$I_2 = \frac{1}{2\pi\theta^{4/3}}\lim_{\alpha\to 0^+}\int_{-\infty - i\alpha}^{\infty - i\alpha} \frac{(i\omega)^{-1/3} e^{i\omega x}\, d\omega}{(i\omega)^{4/3} + \theta^{4/3} i\,\mathrm{sgn}\,\omega}. \tag{43}$$

We note that the integral in Eq. (43) does not contain a branch point. Thus, following steps similar to those used in the case p_∞, we can rewrite Eq. (43) as

$$I_2 = -\frac{3}{\pi\theta^2}\int_0^\infty \frac{\rho}{\rho^8 + 1} e^{-\rho^3\theta|x|}\, d\rho, \quad \text{for } x < 0, \tag{44}$$

$$I_2 = -\frac{3}{2\pi\theta^2}\int_0^\infty \frac{\sqrt{3}\rho^5 - \rho}{\rho^8 - \sqrt{3}\rho^4 + 1} e^{-\rho^3\theta x}\, d\rho, \quad \text{for } x > 0. \tag{45}$$

The integrand in Eq. (42) has a branch point at the origin as well as a branch cut. For $x > 0$, using Cauchy's theorem, we can continuously deform the contour of integration to the Hankel contour shown in Fig. 3. Hence,

$$I_1 = -\frac{1}{2\pi}\int_D \frac{e^{i\omega x}\, d\omega}{(i\omega)^{5/3}\theta^{4/3}}, \tag{46}$$

where D starts from ∞ along the positive imaginary axis, encircles the origin once in the counterclockwise sense, and returns to its starting point. It follows from Appendix A that

$$I_1 = -x^{2/3}/\theta^{4/3}\Gamma(\tfrac{5}{3}) \quad \text{for } x > 0, \tag{47}$$

where Γ is the gamma function.[12] For $x < 0$, we use Cauchy's theorem and deform the contour of integration into the contour $C = C_1 \cup C_2 \cup C_3$, where $C_1 = [-\epsilon_1 - \infty i,\ -\epsilon_1 - \alpha i]$, $C_2 = [-\epsilon_1 - i\alpha,\ \epsilon_1 - i\alpha]$, and $C_3 = [\epsilon_1 - \alpha i,\ \epsilon_1 - \infty i]$ with ϵ_1 being a small positive number. We note that the negative imaginary axis is not a branch cut and the integrand in Eq. (46) is analytic on it. Hence, evaluating I_1 along this contour and taking the limit as $\epsilon_1\to 0$, we find that $I_1 = 0$.

FIG. 3. Hankel contour of integration.

Substituting for I_1 and I_2 in Eq. (41) yields

$$\delta_\infty = -\frac{3}{\pi\theta^2}\int_0^\infty \frac{\rho}{\rho^8 + 1} e^{-\rho^3\theta|x|}\, d\rho, \quad \text{for } x < 0, \tag{48}$$

$$\delta_\infty = -\frac{x^{2/3}}{\theta^{4/3}\Gamma(\frac{5}{3})} - \frac{3}{2\pi\theta^2}\int_0^\infty \frac{\sqrt{3}\rho^5 - \rho}{\rho^8 - \sqrt{3}\rho^4 + 1} e^{-\rho^3\theta x}\, d\rho, \quad \text{for } x > 0. \tag{49}$$

C. Lower-deck streamwise velocity

Using Eq. (32b) and taking the inverse Fourier transform of Eq. (27), we find that

$$u_\infty = -\frac{3}{2\pi}\lim_{\alpha\to 0^+}\int_{-\infty - i\alpha}^{\infty - i\alpha} \frac{i(i\omega)^{-4/3}\,\mathrm{sgn}\,\omega e^{i\omega x}}{(i\omega)^{4/3} + i\theta^{4/3}\,\mathrm{sgn}\,\omega} \times \int_0^y \mathrm{Ai}[(i\omega)^{1/3} t\,]\, dt\, d\omega. \tag{50}$$

Again, the integrand in Eq. (50) has a branch point at the origin and a branch cut. Using partial fractions, we split the integral in Eq. (50) into two integrals and obtain

$$u_\infty = I_1 + I_2, \tag{51}$$

where

$$I_1 = -\frac{3}{2\pi\theta^{4/3}}\lim_{\alpha\to 0^+}\int_{-\infty - i\alpha}^{\infty - i\alpha} \frac{e^{i\omega x}}{(i\omega)^{4/3}} \times \int_0^y \mathrm{Ai}[(i\omega)^{1/3} t\,]\, dt\, d\omega, \tag{52}$$

$$I_2 = \frac{3}{2\pi\theta^{4/3}}\lim_{\alpha\to 0^+}\int_{-\infty - i\alpha}^{\infty - i\alpha} \frac{e^{i\omega x}}{(i\omega)^{4/3} + i\theta^{4/3}\,\mathrm{sgn}\,\omega} \times \int_0^y \mathrm{Ai}[(i\omega)^{1/3} t\,]\, dt\, d\omega. \tag{53}$$

The integrand in I_2 does not have branch points and it is regular at the origin. Hence, we put $\alpha = 0$ in Eq. (53) and rewrite it as

$$I_2 = \frac{3}{2\pi\theta^{4/3}}\int_0^\infty \frac{e^{i\omega x} e^{-i\pi/2}}{\omega^{4/3} e^{i\pi/6} + \theta^{4/3}} \int_0^y \mathrm{Ai}[e^{i\pi/6}\omega^{1/3} t\,]\, dt\, d\omega + \frac{3}{2\pi\theta^{4/3}}\int_0^\infty \frac{e^{-i\omega x} e^{i\pi/2}}{\omega^{4/3} e^{-i\pi/6} + \theta^{4/3}} \int_0^y \mathrm{Ai}[e^{-i\pi/6}\omega^{1/3} t\,]\, dt\, d\omega. \tag{54}$$

We let $\eta = \omega^{1/3} t \exp(i\pi/6)$ and $\eta = \omega^{1/3} t \exp(-i\pi/6)$ in the first and second integrals, respectively, put $\omega = r^3\theta$, and obtain

$$I_2 = \frac{9}{2\pi\theta^2}\int_0^\infty \frac{r e^{ir^3\theta x} e^{-2i\pi/3}}{1 + r^4 e^{i\pi/6}} \int_0^{e^{i\pi/6} r\theta^{1/3} y} \mathrm{Ai}(\eta)\, d\eta\, dr + \frac{9}{2\pi\theta^2}\int_0^\infty \frac{r e^{-ir^3\theta x} e^{2i\pi/3}}{1 + r^4 e^{-i\pi/6}} \int_0^{e^{-i\pi/6} r\theta^{1/3} y} \mathrm{Ai}(\eta)\, d\eta\, dr. \tag{55}$$

We consider the same closed contour we used for the pressure.

For $x<0$, Eq. (55) can be rewritten as

$$I_2=\frac{9}{2\pi\theta^2}\int_0^{\infty}\frac{re^{-ir^3\theta|x|}e^{-2i\pi/3}}{1+r^4e^{i\pi/6}}\int_0^{e^{i\pi/6}r\theta^{1/3}y}\mathrm{Ai}(\eta)d\eta dr+\frac{9}{2\pi\theta^2}\int_0^{\infty}\frac{re^{ir^3\theta|x|}e^{2i\pi/3}}{1+r^4e^{-i\pi/6}}\int_0^{e^{-i\pi/6}r\theta^{1/3}y}\mathrm{Ai}(\eta)d\eta\,dr. \tag{56}$$

We rotate the contour of integration by $-\pi/6$ and let $r=\rho\exp(-i\pi/6)$ in the first integral, rotate the contour of integration by $\pi/6$ and let $r=\rho\exp(i\pi/6)$ in the second integral, combine the results, and obtain

$$I_2=-\frac{9}{\pi\theta^2}\int_0^{\infty}\frac{\rho}{\rho^8+1}\int_0^{\rho\theta^{1/3}y}\mathrm{Ai}(\eta)d\eta\,e^{-\rho^3\theta|x|}\,d\rho\quad\text{for } x<0. \tag{57}$$

For $x>0$, Eq. (55) gives

$$I_2=\frac{9}{2\pi\theta^2}\int_0^{\infty e^{i\pi/6}}\frac{re^{ir^3\theta x}e^{-2i\pi/3}}{1+r^4e^{i\pi/6}}\int_0^{e^{i\pi/6}r\theta^{1/3}y}\mathrm{Ai}(\eta)d\eta\,dr+\frac{9}{2\pi\theta^2}\int_0^{\infty e^{-i\pi/6}}\frac{re^{-ir^3\theta x}e^{2i\pi/3}}{1+r^4e^{-i\pi/6}}\int_0^{e^{-i\pi/6}r\theta^{1/3}y}\mathrm{Ai}(\eta)d\eta\,dr \tag{58}$$

according to Cauchy's theorem. We let $r=\rho\exp(i\pi/6)$ in the first integral and $r=\rho\exp(-i\pi/6)$ in the second integral and obtain

$$I_2=\frac{9}{2\pi\theta^2}\int_0^{\infty}\frac{\rho e^{-i7\pi/6}}{\rho^4+e^{i7\pi/6}}\int_0^{e^{i\pi/3}\rho\theta^{1/3}y}\mathrm{Ai}(\eta)d\eta\,e^{-\rho^3\theta x}\,d\rho+\frac{9}{2\pi\theta^2}\int_0^{\infty}\frac{\rho e^{i7\pi/6}}{\rho^4+e^{-i7\pi/6}}\int_0^{e^{-i\pi/3}\rho\theta^{1/3}y}\mathrm{Ai}(\eta)d\eta\,e^{-\rho^3\theta x}\,d\rho$$

$$\text{for } x>0. \tag{59}$$

To evaluate the integral I_1 when $x>0$, we let $i\omega x=\xi$ and $(i\omega)^{1/3}t=\eta$ and obtain

$$I_1=-\frac{3x^{2/3}}{2\pi i\theta^{4/3}}\lim_{\alpha\to0^+}\int_{-i\infty+\alpha x}^{i\infty+\alpha x}\frac{e^{\xi}}{\xi^{5/3}}\int_0^{y(\xi/x)^{1/3}}\mathrm{Ai}(\eta)d\eta\,d\xi. \tag{60}$$

Using Cauchy's theorem, we continuously deform the contour of integration for ξ in Eq. (60) into the Hankel contour C that starts at the point $-\infty$ on the real axis, encircles the origin once counterclockwise, and returns to its starting point. The contour C is the contour D shown in Fig. 3 rotated by $\frac{1}{2}\pi$. Hence, we rewrite Eq. (60) as

$$I_1=-\frac{3x^{2/3}}{2\pi i\theta^{4/3}}\int_C\frac{e^{\xi}}{\xi^{5/3}}\int_0^{y(\xi/x)^{1/3}}\mathrm{Ai}(\eta)d\eta\,d\xi. \tag{61}$$

For $x<0$, we use Cauchy's theorem and continuously deform the contour of integration in Eq. (52) into the contour $C_1\cup C_2\cup C_3$, where $C_1=[-\epsilon_1-\infty i,\ -\epsilon_1-\alpha i]$, $C_2=[-\epsilon_1-i\alpha,\epsilon_1-i\alpha]$, and $C_3=[\epsilon_1-\alpha i,\epsilon_1-\infty i]$. Since the integrand is analytic on the negative imaginary axis,

$$I_1=0,\quad\text{for } x<0. \tag{62}$$

D. Lower-deck normal velocity

It follows from Eq. (20b), that

$$v_{\infty}=-p_{\infty x}+u_{\infty yy}-yu_{\infty x}. \tag{63}$$

For $x>0$, substituting Eqs. (39), (51), (59), and (61) into Eq. (63) yields

$$v_{\infty}=-\frac{3}{\pi}\int_0^{\infty}\left(1+\frac{3}{\theta^{4/3}}\mathrm{Ai}'(\rho\theta^{1/3}y)-\frac{3y\rho}{\theta}\int_0^{\rho\theta^{1/3}y}\mathrm{Ai}(\eta)d\eta\right)\frac{\rho^3}{\rho^8+1}e^{-\rho^3\theta|x|}\,d\rho. \tag{64}$$

For $x>0$, substituting Eqs. (38), (51), (59), and (61) into Eq. (63) yields

$$v_{\infty}=\frac{3}{2\pi}\int_0^{\infty}\frac{\rho^3}{\rho^8-\sqrt{3}\rho^4+1}e^{-\rho^3\theta x}\,d\rho-\frac{3}{2\pi i}\frac{1}{\theta^{4/3}}\left[\int_0^{\infty e^{i\pi}}\frac{e^{\xi}}{\xi}\mathrm{Ai}'\left(\frac{\xi^{1/3}y}{x^{1/3}}\right)d\xi+\int_{\infty e^{-i\pi}}^{0}\frac{e^{\xi}}{\xi}\mathrm{Ai}'\left(\frac{\xi^{1/3}y}{x^{1/3}}\right)d\xi\right]$$

$$-\frac{9i}{2\pi\theta^{4/3}}\int_0^{\infty}\frac{\rho^3}{\rho^4+e^{i7\pi/6}}\mathrm{Ai}'(e^{i\pi/3}\rho\theta^{1/3}y)e^{-\rho^3\theta x}\,d\rho+\frac{9i}{2\pi\theta^{4/3}}\int_0^{\infty}\frac{1}{\rho^4+e^{-i7\pi/6}}\mathrm{Ai}'(e^{-i\pi/3}\rho\theta^{1/3}y)e^{-\rho^3\theta x}\,d\rho$$

$$-\frac{9y}{2\pi\theta}\int_0^{\infty}\left(\frac{1}{\rho^4+e^{i7\pi/6}}\int_0^{e^{i\pi/3}\rho\theta^{1/3}y}\mathrm{Ai}(\eta)d\eta+\frac{1}{\rho^4+e^{-i7\pi/6}}\int_0^{e^{-i\pi/3}\rho\theta^{1/3}y}\mathrm{Ai}(\eta)d\eta\right)e^{-\rho^3\theta x}\,d\rho. \tag{65}$$

E. Finite-length strip

Let x^*_{LE} and x^*_{TE} denote the dimensional leading and trailing edges of a strip. Appealing to the linearity of Eqs. (20) and (21) and using translations and superpositions of semi-infinite solutions, we obtain

$$u = u_\infty\{[(x^* - x^*_{LE})/x^*_{LE}]\lambda^{5/4}_{LE} U_e^{-3/4}\,\mathrm{Re}^{3/8}_{LE}, y\} - u_\infty\{[(x^* - x^*_{TE})/x^*_{TE}]\lambda^{5/4}_{TE} U_e^{-3/4}\,\mathrm{Re}^{3/8}_{TE}, y\}, \tag{66}$$

with similar corresponds for p, δ, and v. These expressions are valid for any strip width in accordance with linearized triple-deck theory, which is an asymptotic theory for very large Reynolds numbers. Since our interest is in the development of expressions for the mean flow over bodies with many suction strips for finite Reynolds numbers, we employ the reference value x^*_r at the middle of the strip; that is,

$$x^*_r = \tfrac{1}{2}(x^*_{LE} + x^*_{TE})$$

instead of the separate reference values x^*_{LE} and x^*_{TE}. Moreover, we replace λ_{LE} and λ_{TE} with the local value of λ and obtain

$$u(x,y) = u_\infty(x - x_{LE}, y) - u_\infty(x - x_{TE}, y), \tag{67}$$

$$p(x) = p_\infty(x - x_{LE}) - p_\infty(x - x_{TE}), \tag{68}$$

$$\delta(x) = \delta_\infty(x - x_{LE}) - \delta_\infty(x - x_{TE}), \tag{69}$$

$$v(x,y) = v_\infty(x - x_{LE}, y) - v_\infty(x - x_{TE}, y), \tag{70}$$

where $u_\infty, p_\infty, \delta_\infty$, and v_∞ are given in the preceding subsections. Here, we have assumed that v^*_w, the dimensional suction rate, is constant over the whole strip. To accommodate varying suction over the strip, we would approximate the suction distribution by steps and just use more translations and superpositions of semi-infinite solutions. Our numerical results obtained from Eqs. (67)–(70) are in better agreement with the solutions of interacting boundary-layer equations than those obtained from Eq. (66). Moreover, the stability[2] of the flow generated from Eqs. (67)–(70) is in better agreement with the experimental results of Reynolds and Saric.[4]

IV. COMPOSITE EXPANSIONS

In the previous sections, we used the method of matched asymptotic expansions to obtain solutions valid in each of the lower, middle, and upper decks. In order to combine all of these solutions into one set of solutions valid everywhere, we form composite expansions[13,14] by adding the three solutions in the three decks and subtracting the common parts (i.e., middle expansion of lower expansion and upper expansion of middle expansion). For parallel stability calculations,[2,3] one needs an expression for u valid to $O(\epsilon)$. Consequently, we include terms to the order ϵ in the following expansions for u.

A. The case of one strip

For the case of one strip, a composite expansion that is valid for all y^* can be expressed in the original dimensional variables as

$$\frac{u^*}{U^*_\infty} = U(\eta) + U_e^{1/2}\,\mathrm{Re}^{1/4}\lambda^{-1/2}\frac{v^*_w}{U^*_\infty}\left[\left(\frac{U'(\eta)}{U'(0)} - 1\right)\times\delta\left(\lambda^{5/4}\frac{x^* - x^*_r}{x^*_r}U_e^{-3/4}\,\mathrm{Re}^{3/8}\right) + u\left(\lambda^{5/4}\frac{x^* - x^*_r}{x^*_r}U_e^{-3/4}\,\mathrm{Re}^{3/8}, y^*\frac{\mathrm{Re}^{5/8}}{x^*_r}U_e^{-1/4}\lambda^{3/4}\right)\right], \tag{71}$$

valid to first order, where u and δ are given by Eqs. (67) and (69), respectively, the prime indicates the derivative with respect to the argument, λ and Re are defined in Eqs. (3b) and (8b), and

$$\eta = y^*(U^*_\infty/x^*\nu^*)^{1/2}.$$

We note that x^* rather than x^*_r has been used in the expression for η so that Eq. (71) would be valid near as well as far away from the strip.

We note that in the expression for u^*/U^*_∞ we find forms of the Airy function contained in u. One could either integrate these expressions numerically or appeal to asymptotic expansions.

B. The case of *n* strips

We consider now n porous strips centered at $x^*_1, x^*_2, \ldots, x^*_n$ and ordered so that $x^*_i < x^*_{i+1}$. We define the Reynolds number at strip i as

$$\mathrm{Re}_i = x^*_i U^*_{\infty i}/\nu^*.$$

Neglecting the influence of all downstream strips, we propose the dimensional flow quantities, denoted by *, in the neighborhood of the nth strip to be

$$\frac{u^*}{U^*_\infty} = U(\eta) + \sum_{i=1}^{n}\mathrm{Re}_i^{1/4}\lambda_i^{-1/2}U_e^{1/2}\frac{v^*_{w_i}}{U^*_\infty}\left[\left(\frac{U'(\eta)}{U'(0)} - 1\right)\times\delta\left(\lambda_i^{5/4}\frac{x^* - x^*_i}{x^*_i}U_e^{-3/4}\,\mathrm{Re}_i^{3/8}\right) + u\left(\lambda_i^{5/4}\frac{x^* - x^*_i}{x^*_i}U_e^{-3/4}\,\mathrm{Re}_i^{3/8}, y^*\frac{\mathrm{Re}_i^{5/8}}{x^*_i}U_e^{-1/4}\lambda_i^{3/4}\right)\right], \tag{72}$$

where u and δ are defined by Eqs. (67) and (69), respectively, and v^*_{wi} is the dimensional suction rate at the ith strip, which is negative for suction.

All the basic profiles involved in Eq. (72) are functions of

$$\eta = y^*(U^*_\infty/\nu^*x^*)^{1/2},$$

with x^* being the local value rather than the strip center.

V. INTERACTING BOUNDARY LAYERS

Following Ragab and Nayfeh,[15] we introduce the dimensionless variables

$$x=\frac{x^*}{L^*},\quad y=\frac{y^*}{L^*},\quad u=\frac{u^*}{U_\infty^*},\quad v=\frac{v^*}{U_\infty^*},$$

$$p=\frac{p^*-p_\infty^*}{\rho_\infty^* U_\infty^{*2}},$$

and define $\mathrm{Re}_\infty=\rho_\infty^* U_\infty^* L/\mu_\infty^*$, where L^* denotes the distance from the leading edge to the center of the first strip. In dimensionless variables, the two-dimensional boundary-layer equations with constant properties are

$$\frac{\partial u}{\partial x}+\frac{\partial v}{\partial y}=0, \tag{73}$$

$$u\frac{\partial u}{\partial x}+v\frac{\partial u}{\partial y}=-\frac{dp}{dx}+\frac{1}{\mathrm{Re}_\infty}\frac{\partial^2 u}{\partial y^2}. \tag{74}$$

For flow over a plate with uniform suction through a porous strip, the boundary conditions are

$$u=0,\quad \text{at } y=0, \tag{75a}$$

$$v=\begin{cases} v_w, & \text{for } x_{\mathrm{LE}}\leqslant x\leqslant x_{\mathrm{TE}},\quad \text{at } y=0,\\ 0, & \text{otherwise,}\end{cases} \tag{75b}$$

$$u\to U_e(x),\quad \text{as } y\to\infty, \tag{75c}$$

$$u=u_0(y),\quad \text{at } x=x_0, \tag{75d}$$

where $u_0(y)$ is the undisturbed flow at $x=x_0$, a point far ahead of x_{LE}, the strip's leading edge, and x_{TE} is the trailing edge of the porous strip. Introducing the Levy–Lees variables

$$\xi=\int_0^x U_e(x)dx,\quad \eta=\frac{U_e(x)y\sqrt{\mathrm{Re}_\infty}}{\sqrt{2\xi}}, \tag{76a}$$

$$F(\xi,\eta)=u/U_e(x),$$

$$V(\xi,\eta)=\frac{2\xi}{U_e(x)}\left(F\frac{\partial\eta}{\partial x}+\frac{v\sqrt{\mathrm{Re}_\infty}}{\sqrt{2\xi}}\right), \tag{76b}$$

we rewrite Eqs. (73) and (74) as

$$2\xi F_\xi+V_\eta+F=0, \tag{77}$$

$$2\xi FF_\xi+VF_\eta+\beta(F^2-1)-F_{\eta\eta}=0, \tag{78}$$

where

$$\beta=-\frac{2\xi}{U_e^3}\frac{dp}{dx}. \tag{79}$$

The boundary conditions transform to

$$F=0,\quad \text{at } \eta=0, \tag{80}$$

$$V=\begin{cases}\dfrac{v_w\sqrt{2\xi\,\mathrm{Re}_\infty}}{U_e(x)}, & \text{for } \xi_{\mathrm{LE}}\leqslant\xi\leqslant\xi_{\mathrm{TE}},\quad \text{at } \eta=0,\\ 0, & \text{otherwise,}\end{cases} \tag{81}$$

$$F\to 1,\ \text{as } \eta\to\infty, \tag{82}$$

$$F=F_0(\eta),\ \text{at } \xi=\xi_0. \tag{83}$$

Equations (77)–(83) are solved using a second-order-accurate, finite-difference, marching scheme. A Newton–Raphson procedure is used to quasilinearize the nonlinear terms, giving the momentum and continuity equations coupled in their linearized form. This is known as the Davis coupled scheme. The viscous displacement thickness

$$\delta=\frac{\sqrt{2\xi}}{U_e(x)\sqrt{\mathrm{Re}_\infty}}\int_0^\infty(1-F)d\eta \tag{84}$$

is iteratively made to equal the inviscid displacement thickness (i.e., the displacement thickness from boundary-layer interaction with the inviscid flow) given by

$$\frac{dy_D}{dx}=\frac{1}{\pi}\int_{\mathrm{LE}}^\infty\frac{p(t)}{x-t}dt, \tag{85}$$

so that

$$\frac{dp}{dx}=-\frac{1}{\pi}\int_{\mathrm{LE}}^\infty\frac{y_D''(t)}{x-t}dt. \tag{86}$$

The wall shear is then found to be

$$\frac{\tau_w}{\tau_{w_0}}=\frac{U_e^2\sqrt{x}}{\alpha\sqrt{\xi}}\left.\frac{\partial F}{\partial\eta}\right|_{\eta=0}, \tag{87}$$

where τ_{w_0} is the Blasius shear and $\alpha=0.46960$.

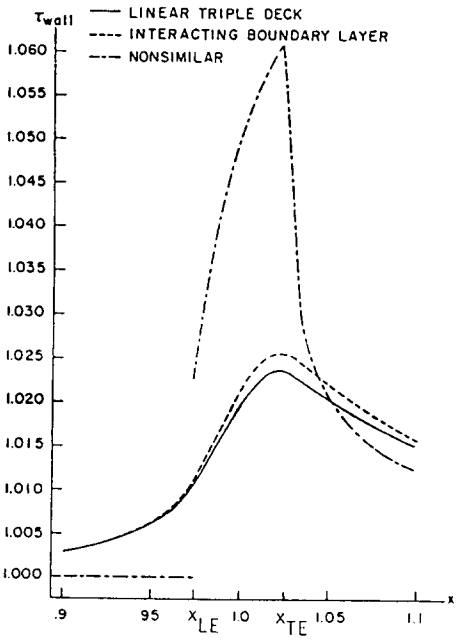

FIG. 4. Wall shear for one strip.

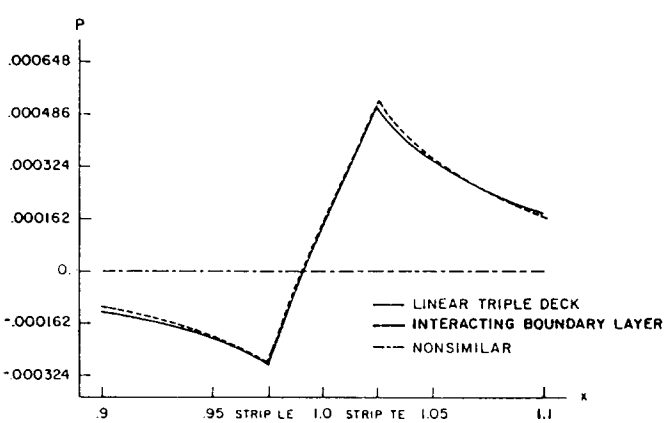

FIG. 5. Wall pressure coefficient for one strip.

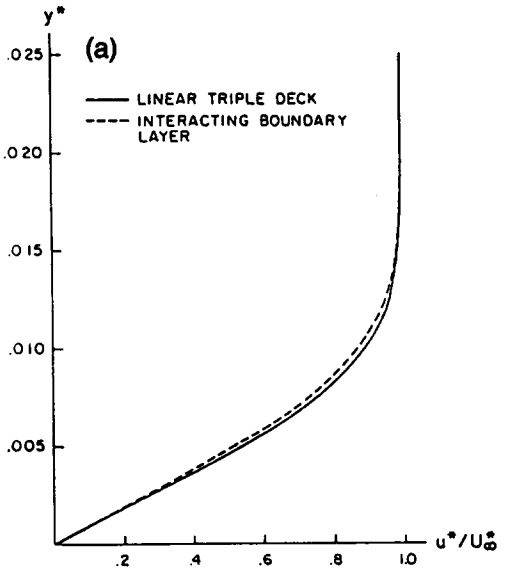

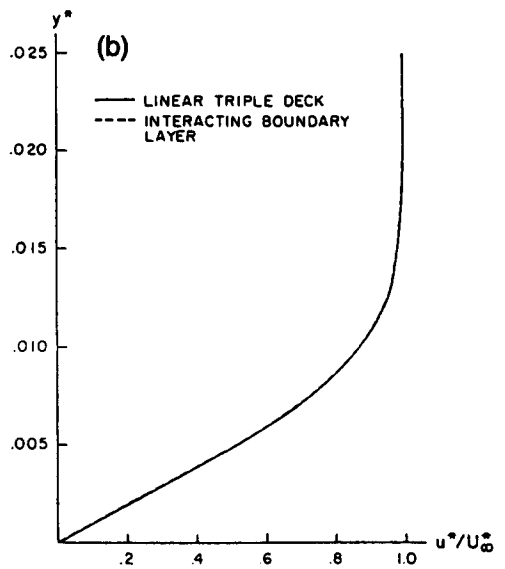

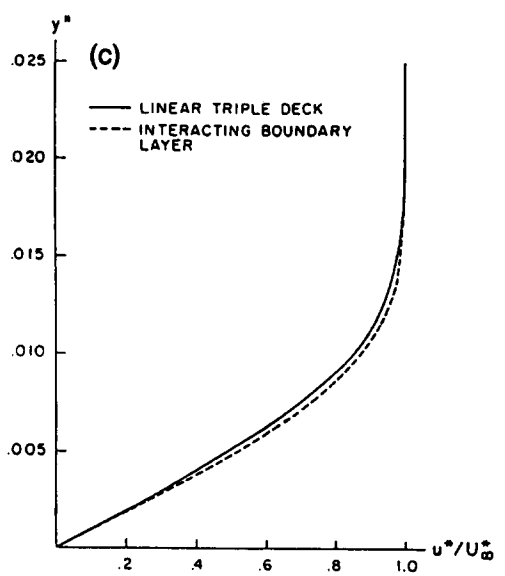

FIG. 6. Streamwise velocity profile at (a) $x^* = 27.432$ cm, upstream of strip; (b) streamwise velocity profile at $x^* = 30.48$ cm, the center of the strip; (c) streamwise velocity profile at $x^* = 33.528$ cm, downstream of suction strip.

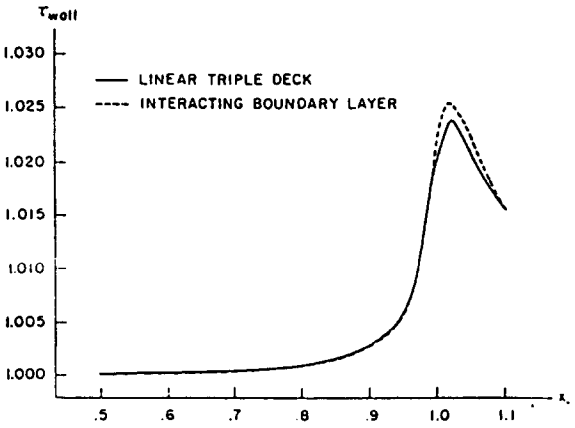

FIG. 7. Upstream influence (wall shear).

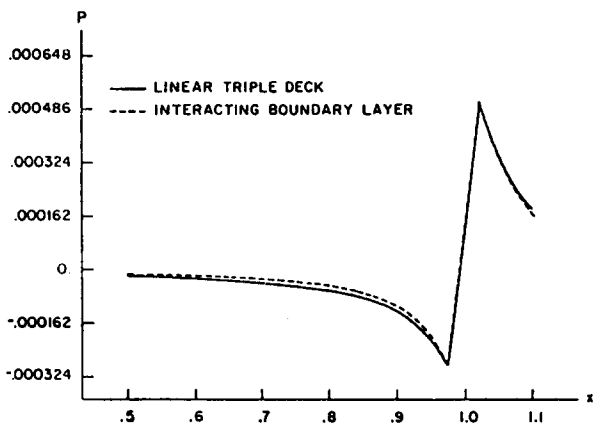

FIG. 8. Upstream influence (wall pressure coefficient).

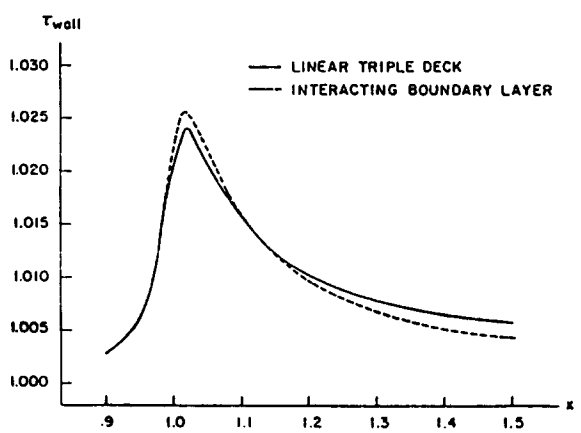

FIG. 9. Downstream influence (wall shear).

VI. COMPARISONS OF THE LINEARIZED TRIPLE-DECK SOLUTIONS WITH INTERACTING-BOUNDARY-LAYER SOLUTIONS

For small injection rates, Napolitano and Messick[9] compared the linearized pressure and wall-shear solutions with two different nonlinear solutions of the triple-deck equations and found excellent agreement in both cases. In this section, we demonstrate the agreement between the linearized solutions and those of the interacting boundary-layer equations for flows past a plate with several porous strips with suction levels and strip widths that are appropriate for laminar flow control.

In order to confirm the validity of the linearized triple-deck solutions, we compare them with the solutions of the interacting boundary-layer equations. The first numerical results given represent the following one-strip configuration:

$$x_r^* = 30.48 \text{ cm}, \quad \mathrm{Re} = \frac{U_\infty^* x_r^*}{\nu_\infty^*} = 1.0\times 10^5,$$

$$v_w^* = -2.3\times 10^{-4} U_\infty^*, \quad \text{strip width} = 0.127 \text{ cm}.$$

Figures 4 and 5 show the normalized wall shear and pressure coefficients, respectively, for the linearized triple deck and the interacting and nonsimilar boundary layers. The agreement between the linearized triple deck and interacting boundary layers is excellent with a maximum error in the wall shear of approximately 0.2% in a neighborhood of the strip. Figures 4 and 5 also show the inaccuracy of the nonsimilar boundary-layer equations resulting from the neglect of the interaction of the viscous and inviscid flows.

Figure 6 shows comparisons between the streamwise velocity components from the linearized triple deck and the interacting boundary layers for the same one-strip configuration as above. It shows excellent agreement between the two profiles at points $x^* = 27.432$ cm upstream of the strip $x^* = 30.48$ cm at the center of the strip, and $x^* = 33.528$ cm downstream of the strip.

In order to analyze the upstream and downstream influences predicted by the linearized theory, we compare the linearized triple deck with both the interacting and the nonsimilar boundary layers. For the same strip configuration as above, Figs. 7 and 8 show that the upstream influence extends to about four strip widths. One strip width corresponds to about sixteen reference boundary-layer thicknesses ($\delta_r = \sqrt{\nu_\infty^* x^*/U_\infty^*}$), so that four strip widths correspond to about 64 reference boundary-layer thicknesses. The upstream influence is practically the same for both the triple deck and the interacting boundary layers, in contrast with the nonsimilar boundary layers that predict zero upstream influence.

Figures 9 and 10 show that the downstream influence extends more than ten strip widths, corresponding to about 160 reference bounday-layer thicknesses. For the linearized triple deck, the decay of the strip's influence is algebraically slower than that predicted by the interacting boundary layers. This discrepancy is inherent in the linearized model. Our assumptions of streamwise variations in the flow quantities being $O(\mathrm{Re}^{-3/8})$ and the strip's influence occurring in a neighborhood $O(\mathrm{Re}^{-3/8} x_r^*)$ of the strip break down when we move far downstream of the strip.

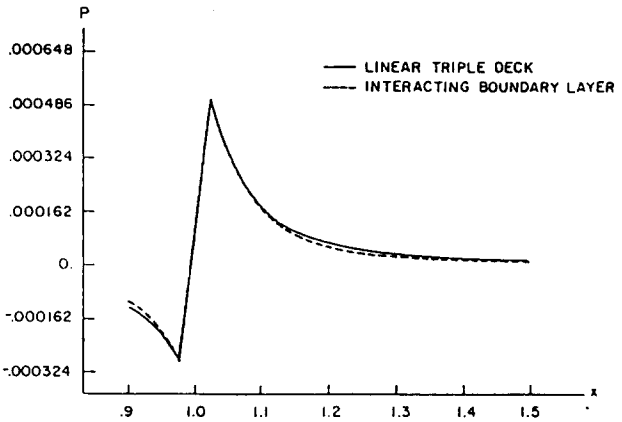

FIG. 10. Downstream influence (wall pressure coefficient).

Comparisons of wall shear and pressure are shown in Figs. 11 and 12, respectively, for the six-strip configuration

$$x_1^* = 30.48 \text{ cm}, \quad x_i^* = x_{i-1}^* + 18.288 \text{ cm},$$

$$\mathrm{Re}_6 = \frac{U_\infty^* x_6^*}{\nu_\infty^*} = 4.0\times 10^5, \quad v_{wi}^* = -2.3\times 10^{-4} U_\infty^*,$$

Strip width = 0.127 cm.

The aforementioned discrepancy in the downstream influence of each of the five superposed upstream strips undoubtedly affects the accuracy of the linearized solutions at the sixth strip. However, the agreement between the linearized triple deck and the interacting boundary layers is entirely satisfactory for practical purposes, the error in the shear being approximately 0.6% in a neighborhood of the sixth strip.

VII. CONCLUSIONS

The linearized triple-deck results are in very good agreement with those of the interacting boundary layers for the wall pressure coefficient, the wall shear, and the streamwise velocity component. Figures 4 and 5 show the inaccuracy of the conventional boundary-layer equations resulting from the neglect of the interaction of the viscous and inviscid flows. These results also show that one can confidently use the linearized triple-deck model to solve accurately for the mean flow over a body with suction through porous strips with suction levels the order of those proposed for laminar

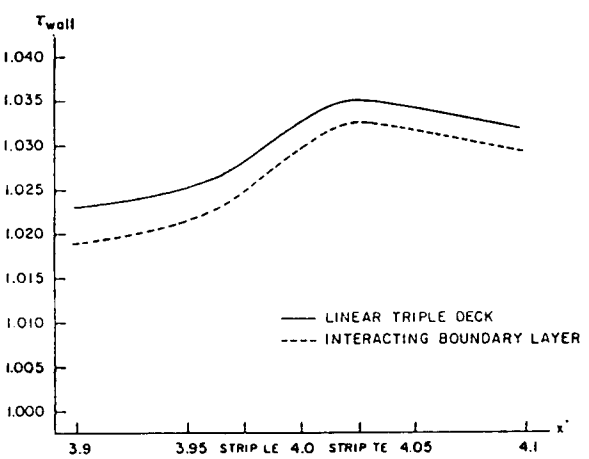

FIG. 11. Wall shear for six strips.

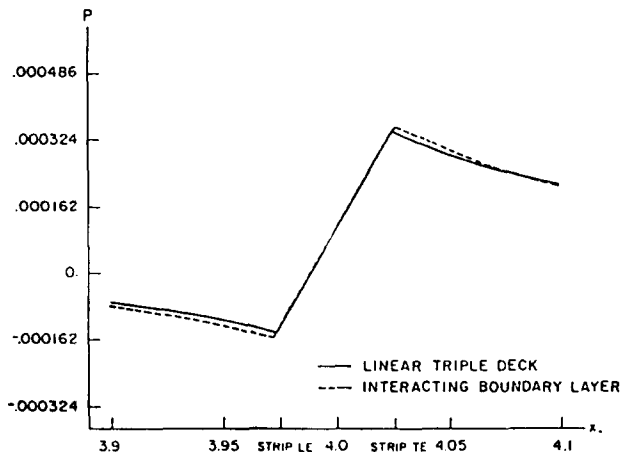

FIG. 12. Wall pressure coefficient for six strips.

flow control $v_w^*/U_\infty = O(10^{-2})$. In fact, the stability of the calculated flows[2] are in good agreement with the experimental results of Reynolds and Saric.[4]

ACKNOWLEDGMENT

This work was supported by the Fluid Dynamics Program of the Office of Naval Research under Contract No. N00014-85-K-0011, NR 432-5201.

APPENDIX: EVALUATION OF THE HANKEL INTEGRAL

To evaluate the integral

$$I = \frac{1}{2\pi} \int_D \frac{(i\omega)^z e^{i\omega x}\, d\omega}{i\theta^{4/3}}, \tag{A1}$$

where $x > 0$, z is a real number, and D is the Hankel contour shown in Fig. 3, we note that $\omega = t \exp(-3i\pi/2)$ along the left cut, $\omega = t \exp(i\pi/2)$ along the right cut, and $\omega = \alpha \exp(i\beta)$ along the circle that includes the origin. Hence, we rewrite Eq. (A1) as the sum of three integrals as

$$I = \frac{1}{2\pi\theta^{4/3}} \int_\infty^\alpha \frac{t^z e^{-t}}{x^{z+1}} e^{-i\pi z}\, dt + \frac{1}{2\pi\theta^{4/3}} \times \int_\alpha^\infty \frac{t^z e^{-t}}{x^{z+1}} e^{i\pi x}\, dt + I_\alpha, \tag{A2}$$

where

$$I_\alpha = \frac{1}{2\pi\theta^{4/3}} \left(\frac{\alpha}{x}\right)^{z+1} \times \int_{-3\pi/2}^{\pi/2} e^{-\alpha x \sin\beta + i(\alpha x \cos\beta + \beta + \pi z/2)}\, d\beta. \tag{A3}$$

As $\alpha \to 0$, $I_\alpha \to 0$ for all values of $z > -1$. Then, I becomes

$$I = \frac{i \sin \pi z}{\pi\theta^{4/3} x^{z+1}} \lim_{\alpha \to 0^+} \int_0^\infty t^z e^{-t}\, dt = \frac{i \sin \pi z}{\pi\theta^{4/3} x^{z+1}} \Gamma(1+z), \tag{A4}$$

where Γ is the gamma function. But $\Gamma(z)\Gamma(1-z) = \pi/\sin \pi z$, thus

$$I = -i/\theta^{4/3} x^{z+1} \Gamma - (z). \tag{A5}$$

Although we have proved Eq. (A5) when $z > -1$, it does hold for all values of z, by the theory of analytical continuation, since the expressions on each side of the equation are analytic functions.[16]

[1] A. H. Nayfeh and N. A. El-Hady, *The 12th Fluid and Plasma Dynamics Conference, Williamsburg, Virginia*, AIAA Paper 79-1494, 1979.
[2] H. L. Reed and A. H. Nayfeh, AIAA J. **24**, 208 (1986).
[3] A. H. Nayfeh and H. L. Reed, Phys. Fluids **28**, 2290 (1985).
[4] G. Reynolds and W. S. Saric, AIAA J. **24**, 202 (1986).
[5] K. Stewartson and P. Williams, Proc. R. Soc. Lond. Ser. A **312**, 181 (1969).
[6] V. Neiland, Izv. Akad. Nauk. SSSR. Mek. Zhid. Gaza **4**, 53 (1969).
[7] A. Messiter, SIAM J. Appl. Math. **18**, 241 (1970).
[8] K. Stewartson, in *Advances in Applied Mechanics* (Academic, New York, 1974), Vol. 14, pp. 145–239.
[9] M. Napolitano and R. E. Messick, Comp. Fluids **8**, 199 (1980).
[10] C. Chester, *Techniques in Partial Differential Equations* (McGraw-Hill, New York, 1971).
[11] P. W. Duck, Q. J. Mech. Appl. Math. **37**, 57 (1984).
[12] M. Abramowitz and I. Stegun, *Handbook of Mathematical Functions* (Dover, New York, 1972).
[13] M. Van Dyke, *Perturbation Methods in Fluid Mechanics* (Parabolic, Stanford, 1975).
[14] A. H. Nayfeh, *Perturbation Methods* (Wiley-Interscience, New York, 1973).
[15] S. A. Ragab and A. H. Nayfeh, in *Numerical and Physical Aspects of Aerodynamic Flows*, edited by T. Cebeci (Springer, New York, 1982), pp. 237.
[16] E. T. Copson, *An Introduction to the Theory of Functions of a Complex Variable* (Oxford U. P., Oxford, 1935), pp. 224–227.